Femtosecond laser fabrication of hybrid micro-optical elements and their integration on the fiber tip

Mangirdas Malinauskas[a], Holger Gilbergs[b], Albertas Žukauskas[a], Kastytis Belazaras[a], Vytautas Purlys[a], Marius Rutkauskas[a], Gabija Bičkauskaitė[a], Andrej Momot[a], Domas Paipulas[a], Roaldas Gadonas[a], Saulius Juodkazis[c], and Algis Piskarskas[a]

[a] Laser Nanophotonics Group, Department of Quantum Electronics, Physics Faculty, Vilnius University, Saulėtekio 9, LT-10222 Vilnius, Lithuania

[b] Institute of Applied Optics, Stuttgart University, Pfaffenwaldring 9, 70569 Stuttgart, Germany

[c] Centre for Micro-Photonics, Faculty of Engineering and Industrial Sciences, Swinburne University of Technology, Hawthorn, VIC, 3122, Australia

ABSTRACT

Femtosecond laser photo-polymerization of zirconium-silicon based sol-gel photopolymer SZ2080 is used to fabricate micro-optical elements with a single and hybrid optical functions. We demonstrate photo-polymerization of the solid immersion and Fresnel lenses. Gratings can be added onto the surface of lenses. The effective refractive index of polymerized structures can be controlled via the volume fraction of polymer. We used woodpile structure with volume fraction of 0.65-0.8. Tailoring of dispersion properties of micro-optical elements by changing filling ratio of polymer are discussed. Direct write approach is used to form such structures on a cover glass and on the tip of an optical fiber. Close matching of refractive indices between the polymer and substrate in visible and near infra red spectral regions ($n_{SZ2080} = 1.504$, $n_{glass} = 1.52$) is favorable for such integration. The surface roughness of laser-polymerized resits was ∼30 nm (min-max value), which is acceptable for optical applications in the visible range. For the bulk micro-optical elements the efficiency of 3D laser polymerization is increased by a factor $\sim (2-4) \times 10^2$ times (depends on the design) by the shell-formation polymerization: *(i)* contour scanning for definition of shell-surface, *(ii)* development for removal of nonfunctional resist, and *(iii)* UV exposure for the final volumetric polymerization of an enclosed volume.

Keywords: nanofabrication; femtosecond laser polymerization; 3D nano-structuring; micro-optics; solid immersion lenses; fiber-optics; control of refractive index.

1. INTRODUCTION

The basic functions of optical macro- and micro-elements are to provide control over light refraction, diffraction, and dispersion at different wavelengths. As optical elements decreases in size as required for integration into optical, mechanical, and fluidic micro-chips new challenges mount in handling and an optical material processing with high sub-wavelength precision of small micro-optical elements. Also, new methods to control light propagation should be implemented as the large angular changes in light propagation (focusing, diffraction, or collimation) should be realized within a small space on a chip or sensor. After an almost decade long demonstration of three-dimensional (3D) capability of photo-polymerization by femtosecond laser pulses, which resulted in endless examples of micro-objects from micro-animals, buildings, logos, the technology of direct laser writing is matured enough to deliver useful solutions for fabrication of micro-optical elements, 3D bio-medical scaffolds for cell culture and implants, fuel cells, and solar cells.

The feature size of photo-polymerization can be smaller than the diffraction limit for the given focusing conditions due to a threshold response of resist and can be made considerably smaller than the wavelength of laser illumination.[1] Originating from rapid prototyping based μ-stereolithography[2] and non-linear optical microscopy[3] a technique of multi-photon polymerization (MPP) reflecting a nonlinear character of absorption required for a 3D structuring emerged a decade ago.[4] Being a direct writing method it offers the most flexible

Further author information: (Send correspondence to M. M.)
M. M.: E-mail: Mangirdas.Malinauskas@ff.vu.lt

Micro-Optics 2010, edited by Hugo Thienpont, Peter Van Daele, Jürgen Mohr, Hans Zappe,
Proc. of SPIE Vol. 7716, 77160A · © 2010 SPIE · CCC code: 0277-786X/10/$18
doi: 10.1117/12.854396

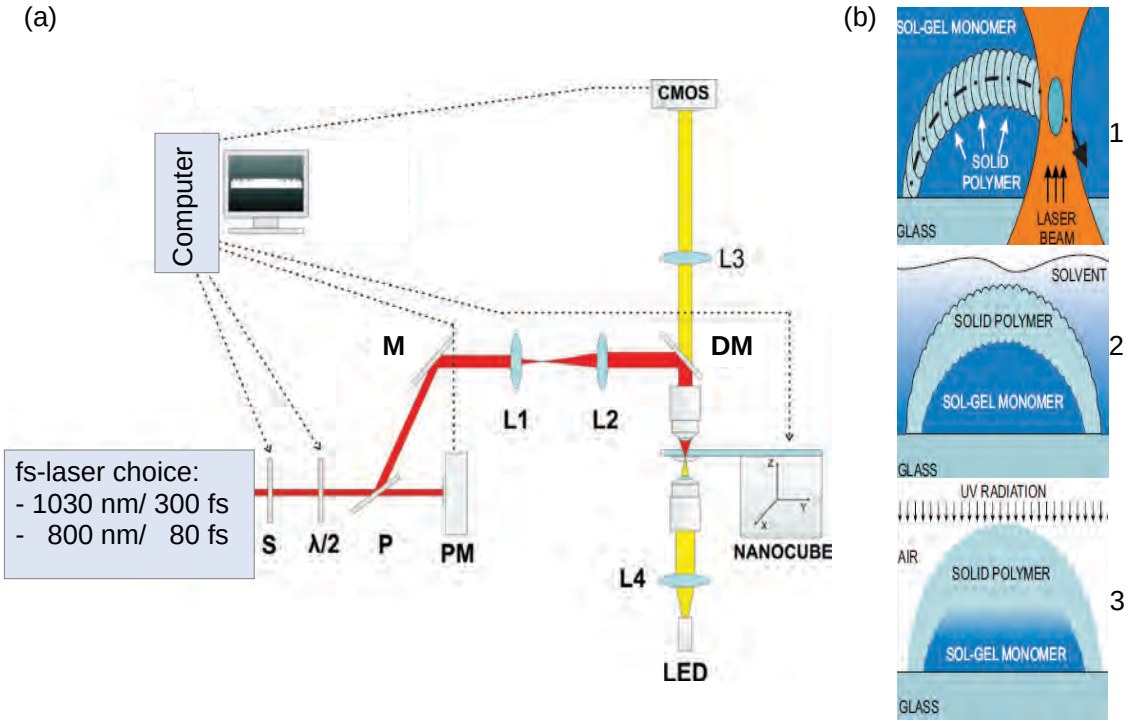

Figure 1. (a) Setup of the *direct laser writing*; PM - powermeter, S - shutter, P - polarizer, M - mirror, DM - dichroic mirror, an alignment telescope made out of pair of L1 and L2 lenses, LED - light emitting diod illumination, $\lambda/2$ - half wave-plate, and CMOS - imaging camera. (b) The used fast polymerization sequence: *(1)* contour scanning for a shell-surface definition, *(2)* development, and *(3)* UV exposure for the final volumetric polymerization. A 3D-Poli software is used for the automation and control of the whole laser fabrication process.

3D structuring of photopolymers at micro- and nanoscale.[5,6] The direct write in polymers is used for fabrication of photonic,[7–11] micro-optical,[12–17] and microfluidic[18,19] devices. New designs of complex miniaturized and integrated optical and opto-fluidic devices and sensors are sought of. As new photo-materials are synthesized and used for laser polymerization, detailed investigations on damage threshold, resolution improvement, and search for methods to increase fabrication throughput evokes further efforts in controllable and reproducible manufacturing of optical components.

To create high quality micro-optical components the photopolymer's properties are playing an important role. Hybrid organic-inorganic materials are expected to dominate this field since they ensure high structuring quality, small achievable feature size, are transparent to visible part of spectrum, their refractive index can be tuned in order to match the required value.[16,20,21] Additionally, these materials can be doped with quantum dots,[22] non-linear chromophores[23] or organic dyes,[24–26] thus further increase their functionality. Low shrinkage of the hybrid resists is favorable for fabrication of micro-optical devices and photonic crystals over larger areas with cross sections above 100 μm without peeling of at the edges. This is due to the fact that the strain, $\varepsilon = \frac{\Delta l}{l}$, for a small lateral shrinkage length Δl over length l would cause the force defined by Hooke's law $F = \varepsilon Y$ and predicts a strong deformation of material with a lower Young modulus, Y, on the polymer-substrate boundary. This is a primary cause of detachment at the periphery of polymerized structures with larger cross-section. SZ2080 structures are prone to a lesser extent to such failure. Also, silica and zirconia glassy structure of polymer makes it compatible with glass substrate for micro-fluidic applications where surface should be hydrophilic.

In this work we show examples of possible hybridization of optical functions into one design of an optical element. This would allow for new light processing within a micro-chip. The refractive index as well as mechanical properties of the photo-polymerized structures can be controlled by changing the volume fraction of the polymerized volume. This also opens new avenues to tailor surface-to-volume ratio of fabricated structures and can be used in sensor and light harvesting applications. The direct write fabrication routine is made faster by a

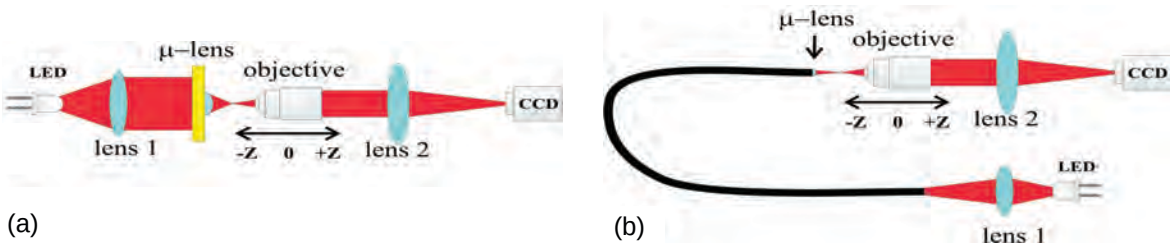

Figure 2. Optical characterization of micro-optical element (a μ-lens) formed on a cover glass (a) and optical fiber tip (b).

factor of $\sim 2 \times 10^2$ (depends on design of an optical element) applying, first, a shell-surface polymerization which separates an internal volume of the optical element from the rest of the resist, secondly development and removal of the non-functional resist, and, finally, an uniform UV exposure to homogenize and solidify the element.

2. SAMPLES AND METHODS

2.1 Materials

We used a commercial hybrid organic-inorganic Zr containing negative photopolymer SZ2080[27] (FORTH, Greece). This resist consists of 20% of zirconia and 80% of polymer forming methacryl-oxypropyl-trimethoxy-silane (MAPTMS, Polysciences Inc.) and methacrylic acid (MAA, Sigma-Aldrich) both having photo-polymerizable methacrylate moieties[28] with different photoinitiators Irgacure 369 (2-Benzyl-2-dimethylamino-1-(4-morpholinophenyl)-butanone-1) and Michler's ketone (4,4'-bis(dimethylamino)benzophenone); referred to as Irg. and Bis., respectively. Detailed description of resist preparation is given in ref.[28] Samples were prepared by drop-casting over a cover glass with subsequent annealing at 100°C for 1-2 h without a post-exposure bake. Figure 3 shows an example of photoluminescence excitation (PLE) spectra of the SZ2080 resist with Irg. photo-sensitizer. Most of lenses shown in this work are made using SZ2080 with Bis. (if not specified otherwise) as it has stronger overall (linear and nonlinear) absorption at the used 800 nm irradiation which is beneficial for efficient fabrication of large surface and volume structures (partly at the expense of reduced resolution). It is noteworthy, that by changing concentration of the photo-initiator within 0.5-2.5 wt.% the required photo-sensitivity of the resist can be flexibly tuned to the requirements of fabrication. More details on optical properties of the used photo-resists and the mechanisms of there structuring by fs-laser pulses can be found elsewhere.[29]

Complex and geometrically discontinuous shapes can be formed as the scanning trajectory of a laser beam focus can be freely chosen and moved with no restrictions. As long as the solubility properties of the solidified and gel state resist are different, the non-polymerized material can be washed away to leave the free-standing structures attached to the substrate. The 4-methyl-2-pentanone (isobutylmethyl ketone) mixed with isopropanol in equal quantities was used as a developer. All chemicals were obtained from Sigma-Aldrich Co. and used directly with no further purification. SZ2080 is known to have low shrinkage and sustain high structural rigidity as well as refractive index is almost matching the one of the glass in visible spectral range ($n_{SZ2080} = 1.504$, $n_{Glass} = 1.52$).[21] This makes this material highly suitable for fabrication of micro-optical and integrated structures.

2.2 Femtosecond formation of 3D micro-optics

Fabrication system is shown in Fig. 1a. A $100^{\times}$ magnification objective lens of numerical aperture $NA = 1.4$ was used (SplanApo, Olympus) in all experiments. The positioning system consists of three stacked micrometer step-motor stages (Standa) and a piezo nano-positioning stage (Nanocube, Physik Instrumente) mounted over. The step-motor stages are used to increase fabrication field were the structures will be localized on the substrate while the piezo stage ensures precise fabrication of the microstructure. The exposure time is controlled by a home-made mechanical shutter with a response time of 5 ms which was adequate for the implemented designs. Wide-field transmission imaging is used to monitor the processing in real time. An optical contrast arises from the different densities and hence indices of refraction upon polymerization. A microscope is built by assembling its main components: a source of red light provided by LED, a CMOS (mvBlueFOX-M102G, Matrix Vision) camera, a video monitor, and the beam delivery optics. The ability to image the sample while performing

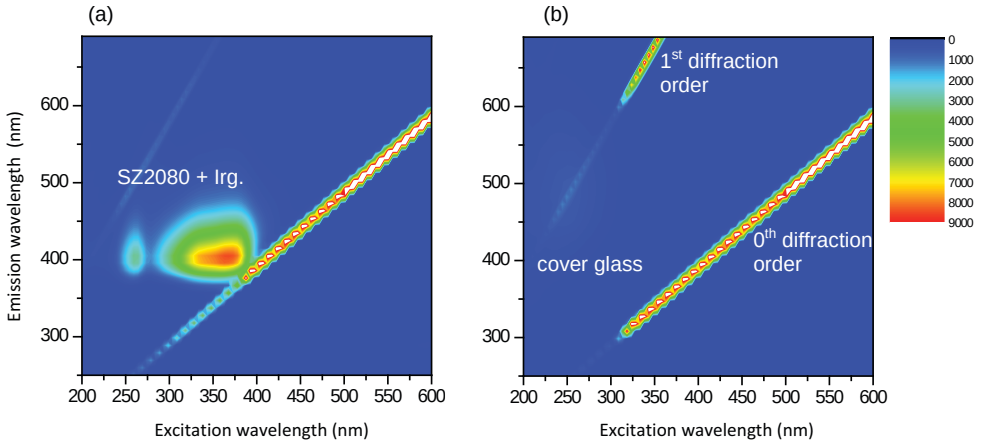

Figure 3. The photoluminescence excitation (PLE) spectra of a drop-casted and dried resist ready for fs-laser structuring (a) and the cover glass (b). The resist is SZ2080 with 2wt.% of Irgacure 369 (2-Benzyl-2-dimethylamino-1-(4-morpholinophenyl)-butanone-1), Irg. for short.

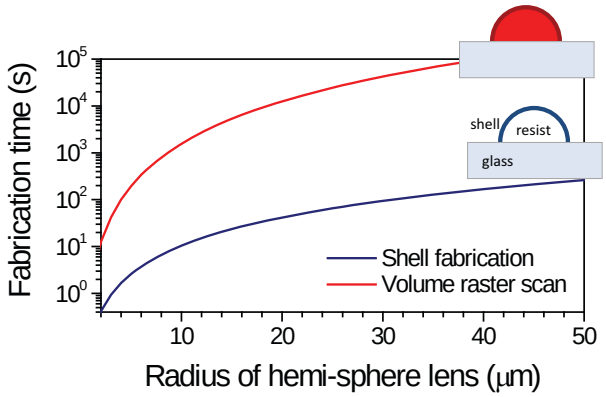

Figure 4. Comparison of time required to fabricate a hemi-spherical lenses of different radii, r, by the proposed shell exposure vs. a full-volume raster scan. The step between exposure spots was $d = 200$ nm, scan speed $v = 100$ μm/s. Curves are calculated by formulas presented in Sec. 2.2.

structuring is an important feature for a successful fabrication process. It is of outmost importance to anchor the microstructures to the substrates to withstand washing step of the unsolidified resin due to capillary force.[30] When required by design, the polymerized regions can be re-exposed as beam is overlayed with the already fabricated region since the polymerized material is still highly transparent to IR laser light. The diameter d and height l of single photo-polymerized volume pixels (voxels) can be controlled by precisely adjusting laser power, exposure time, and focusing optics.[31,32] This allowed to create mechanically strong enough enclosure shell and form surface with unexposed regions inside the optical element for further processing steps schematically depicted in Fig. 1b.

The used procedure of shell formation, development, and then homogenization under UV exposure have speeded up the entire procedure of formation of optical element by a factor of approximately ~ 200. The time required to fabricate a hemi-spherical lens of radius, r, by volumetric raster scanning with pitch, d, (the same pitch in lateral and axial directions is considered) at scan speed, v, is: $t_v = \frac{V}{d^2 v}$ where the volume of hemi-sphere $V = \frac{1}{2} \times 4\pi r^3$; the pitch is at least twice smaller than cross section of the voxel actual fabrication. For the shell fabrication the required time is $t_s = \frac{S}{dv}$ with the surface of hemi-sphere $S = \frac{1}{2} \times \frac{4}{3}\pi r^2$. Hence, the factor of the efficiency increase is $f_c \equiv \frac{t_v}{t_s} = 3\frac{r}{d}$. As radius of a lens increases or voxel size decreases (hence, the pitch, d, too), the time of fabrication becomes impractical for the volumetric raster fabrication. In case of micro-optical elements discussed in this study an improvement of approximately $(1-3) \times 10^2$ times is achieved using shell-fabrication approach as shown in Fig. 4. The actual time of exposure required for a lens of $r = 50$ μm diameter

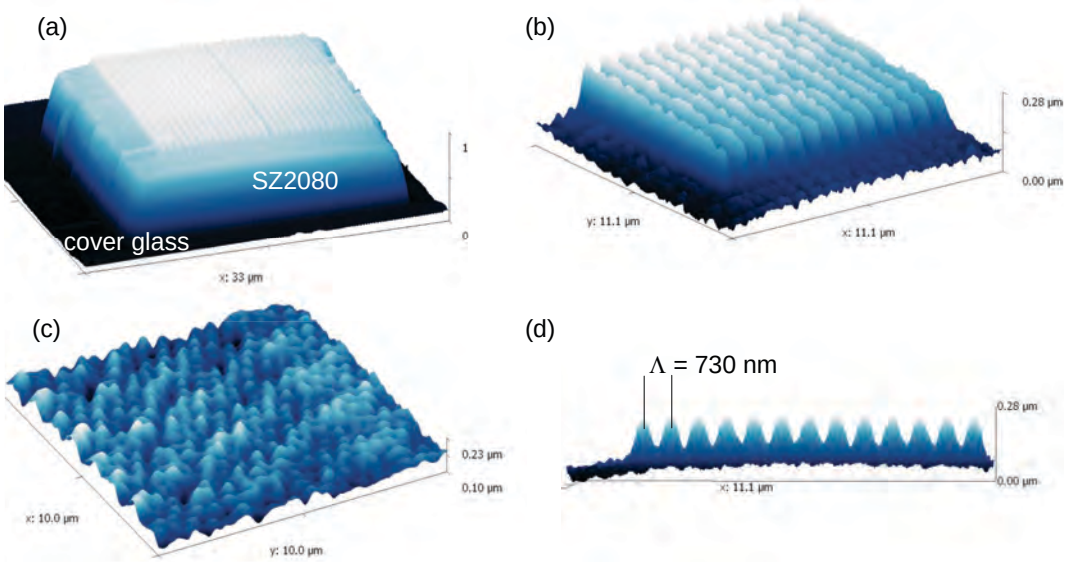

Figure 5. (a) AFM profiles of a grating photo-polymerized by 800 nm/80 fs pulses in SZ2080 resist; (b) a close up view. (c) Surface roughness of a fs-laser polymerized SZ2080. (d) Side view of the grating profile.

and focal length 200 μm at raster scanning with 200 nm overlap between voxels is 880 min, but shell-exposure (Fig. 1b) only ~ 2.6 min is required. Moreover, further optimization is possible if a Fresnel lens design is adopted as the volume of optical element is reduced.

Femtosecond laser light source is a Yb:KGW solid-state laser Pharos (Light Conversion) operating at 1030 nm wavelength with 300 fs pulses. An 100 nm spatial overlap of neighboring pulses corresponding to a scan speed is 100 μm/s. A spherical aberration due to refractive index mismatch between immersion oil ($n = 1.515$) and cover glass substrate is negligible and a spherical aberration-free structuring conditions exist for the focusing depths up to ~ 30 μm.[33]

We also used a femtosecond mode-locked Ti:Sapphire (Spectra Physics) laser emitting 80 fs pulses at repetition rate of 80 MHz and having a central wavelength fixed at 800 nm. At high laser power of 24 mW (at the monitoring point as shown in Fig. 1), a polymerization of the entire micro-lens volume is achieved when a height of the lens dome is less than the axial length of the voxel for the 100 μm/s scan speed. At a 12 mW power, the inner volume of the micro-lens contains an unpolymerized resist. The minimum successful fabrication laser power was 10 mW, while for the lower powers the shell was mechanically unstable and was always damaged during development. A large fs-laser repetition rate increase efficiency of overall fs-writing step, however, more stringent requirements for control of shutter, stage movement, acceleration and deceleration, pulse overlap and over-exposure become apparent. It is noteworthy, that at tens-of-MHz repetition rate thermal accumulation become significant and can be well exploited for efficient polymerization which proceeds via nonlinear absorption and avalanche[29] in the case of low repetition rate.

2.3 Optical and surface inspection

The focal length of fabricated lenses is from several tens to hundreds of micrometers. For measuring such small focal distances we used a microscope setup mounted on a micrometer step-motor with step size of 2.5 μm (Standa) as shown in Fig. 2a. As stage moves, the focal plane of the microscope scans through the focus of the fabricated micro-lens, which is illuminated by a collimated light from a light emitting diode (LED) and an image of the light distribution is captured on a CCD camera. The images are analyzed by fitting a Gaussian function to the acquired light distribution. The width of the Gaussian is evaluated, thus the smallest indicating the focal position of the lens. The same approach is used for fiber-integrated micro-lenses (Fig. 2b).

We fabricate spherical lenses with different radius of curvature and therefore different focal length. The glass surface was considered as the reference surface for the focal distance measurement by the experiment described

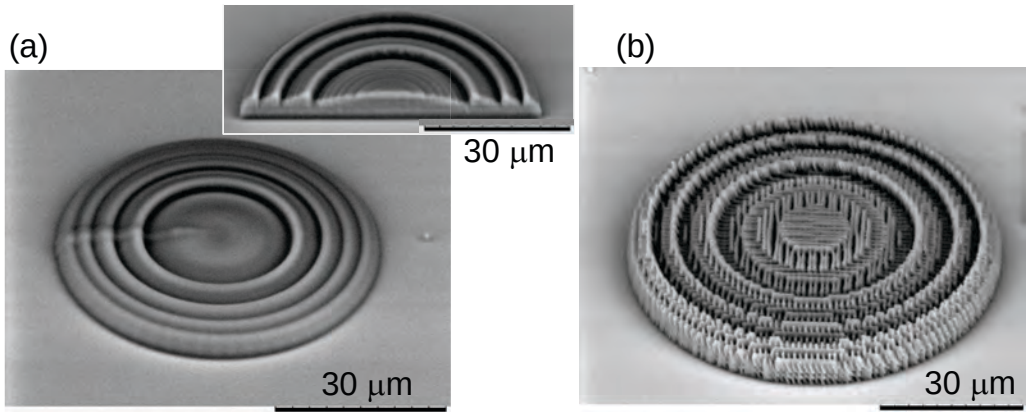

Figure 6. (a) SEM image of a Fresnel lens formed by the fast polymerization sequence on a cover glass. Inset shows half-of the lens. (b) Hybrid Fresnel lens and woodpile structure formed by imposing Fresnel lens spatial profile over the photonic crystal template. The filling ratio of polymer is $f_{polym.} \simeq 0.70 \pm 0.05$.

above and applying thickness of the lens (production parameter) as an offset. For a validation test spherical lenses were fabricated and compliance with the expected focal length which should be twice the radius of curvature was performed.

Optical profilometer (PLμ2300, Sensofar) and atomic force microscopy (AFM: Dimension 3100, Digital Instruments) were used to characterize geometry of the surface, its nano-structure and roughness. Scanning electron microscopy (SEM) was used for sample inspection. Photoluminescence (PL) and its excitation (PLE) spectra were employed for characterization of resist.

3. RESULTS AND DISCUSSION

3.1 Single optical elements: grating and lenses

Figure 5 shows AFM profiles of a photo-polymerized grating. Grating period, Λ, has been chosen to be smaller than the wavelength $\lambda = 800$ nm of fs-laser irradiation. The grating structure has approximately 140 nm depth. The grating is recorded by a single scan at the height augmented by 50 nm above the polymerized surface. Laser beam has an approximate diameter of $2r = 1.22\lambda/NA \simeq 697$ nm for the employed focusing conditions. The retrieved grating with period comparable with the focal spot size is fabricated (see, Fig. 5(d)). Such surface relief patterns with feature sizes close to 100 nm are prospective for optical designs where near-field effects are exploited, e.g., for plasmonic applications.

The surface roughness average across the polymerized surface is typically $\sim 30 \pm 3$ nm (Fig. 5), which is already in the range of a tenth of an optical wavelength in the visible spectral range. The roughness of $\sim$5 nm is due to the minimal clusters formed during fabrication and development process. Such roughness is acceptable for optical devices such as gratings and micro-lenses.

In order to minimize structural distortions of photo-polymerized optical elements and to make fabrication sequence fast and practical, the amount of volume which should be exposed using a direct write approach should be minimized. Function of a volumetric micro-lens[15] can be realized by a micro-Fresnel lens (Fig. 6) which occupies a smaller volume and, hence, has advantages for integration into micro-electro-mechanical systems MEMS and their optical counterparts MOEMS or micro-fluidic chips. The used shell-formation approach without lengthy raster-scanning of entire volume (Fig. 1a) serves this purpose. The entire laser exposure process of micro-lens is reduced by a factor of $f_c \simeq 880/2.62 = 335$ as described in Sec. 2.2.

Solid immersion lenses (SIL) are spherical plano-convex lenses that can be used to increase the numerical aperture, as well as the magnification of a microscope objective.[34] SILs offers advantageous possibilities for microscopic and spectroscopic applications, especially when liquid immersion techniques with water or oil can not be used, e.g., at temperatures below the solidification temperature of the liquid immersion medium.

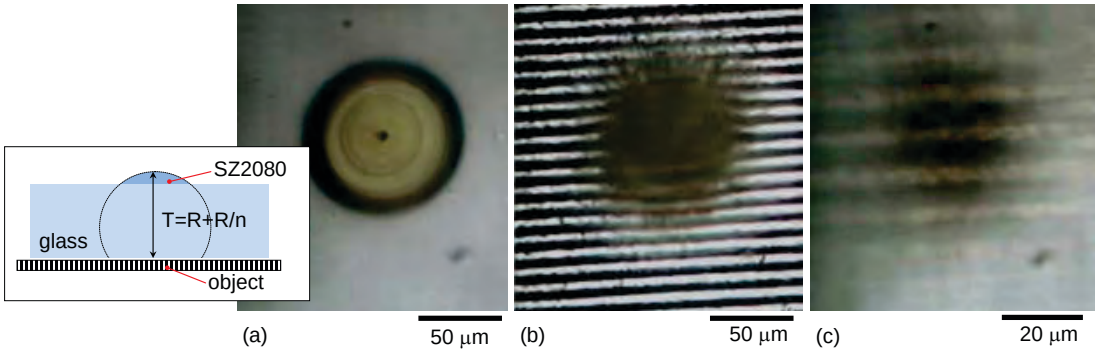

Figure 7. (a) Top-optical view of the polymerized Weierstrass-sphere solid immersion lens (SIL). The inset shows the design where truncation, T, is defined by the radius, R, and refractive index, n, as $T = R + R/n$. (b) Top-view of the micrometer grid (the imaging object shown in inset of (a)). (c) The image of the scale through polymerized SIL. All images were taken with the same objective lens (Olympus plan FL N $10^{\times}0.25$).

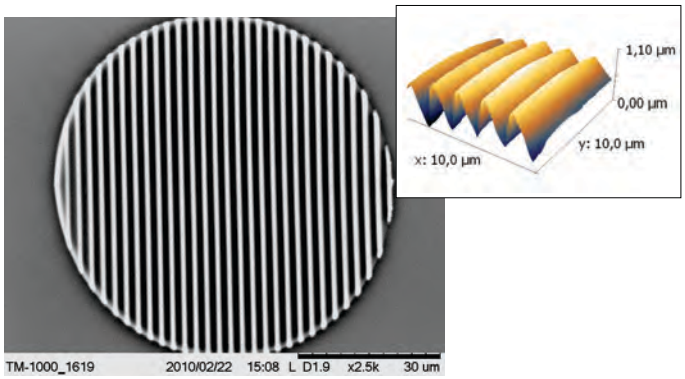

Figure 8. SEM image of a hybrid micro-lens with a phase grating. The curvature radius of the lens is $R = 67$ μm, grating period $d = 2.4$ μm. Inset shows a profile measured by AFM (Scanning probe, AFM dimension 3100, Digital Instruments).

SILs increase the numerical aperture of an imaging system in two different ways. Firstly, The NA depends linearly on the refractive index n_{SIL}. SILs that have a half-sphere geometry rely on this effect, refraction on the surface is kept minimal as the incident angle on the lens is nearly 90° degrees. The optical path length inside the medium is also constant, so chromatic aberration is minimal. The second way to increase the NA is by using the refraction on the surface of the SIL to increase the opening angle. Typically a Weierstrass-sphere geometry (a sphere of radius R with refractive index n_{SIL} truncated to a thickness T of $T = R + R/n_{SIL}$) is applied as it does not introduce additional spherical aberrations into the optical system.[35] Because this geometry uses both effects the increase of the numerical aperture is greater than the one of the half-sphere SIL and $NA \propto n_{SIL}^2$.

The second effect that solid immersion lenses have on optical imaging is the increase in magnification. It depends on the refractive index n_{SIL} of the lens, its radius of curvature R and its center thickness T:

$$M' = M \times \frac{n_{SIL}}{\frac{T-R}{R}(1 - n_{SIL}) + 1}. \tag{1}$$

For a hemispherical SIL when $T = R$ the numerical aperture as well as the magnification is increased by a factor of n_{SIL}, the refractive index of the lens material. For a Weierstrass-sphere SIL the increment factor equals n_{SIL}^2 as follows from eqn. 1.

Figure 7 shows the design and performance of the polymerized Weierstrass-sphere type SIL. SIL is made by only polymerizing the top part of the lens (see, inset in Fig. 7a). A combination of the cap and glass-substrate functions as a SIL is due to a good matching of the refractive indexes between the SZ2080 polymer (1.504) and the the cover glass ($n = 1.52$). The curvature radius of a Weierstrass-sphere SILs is 92 μm, the thickness of the glass substrate is 144 ± 1 μm. The manufactured polymer cap has a center height of about 12 μm and a diameter of 93 μm.

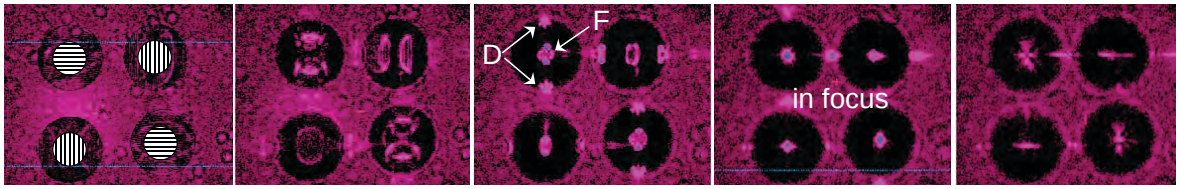

Figure 9. Imaging of the light passed through an array of 2×2 of hybrid microlens-phase grating components at different distances from the cover glass surface as indicated. The orientation of gratings is shown schematically on the left-side image. The curvature radius is 67 μm; diameter 90 μm. Focus position at $\sim$ 120 μm distance from the surface of cover glass. The marks D and F denote diffracted and focused beams, respectively.

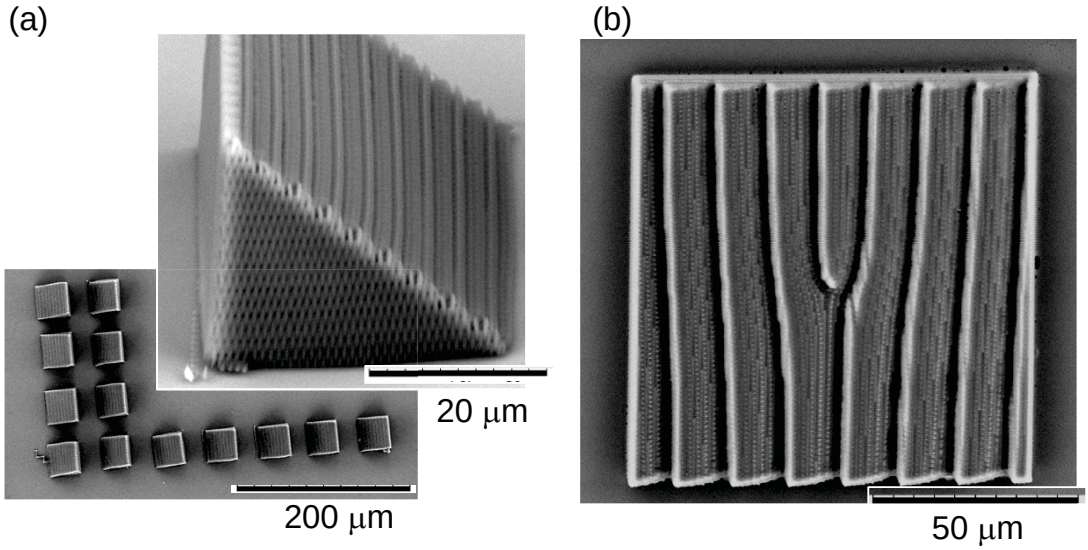

Figure 10. (a) SEM image of a large area (with cross section $\sim$ 1 mm) patterned by woodpile-structured prisms. Inset shows a close up view of a single prism. (b) A hybrid optical vortex generating grating made out of a woodpile template with a gradual phase change over the period. The filling ratio of polymer is $f_{polym.} \simeq 0.80 \pm 0.05$; can be varied within 0.6-0.8 range using a standard wet bath development procedure.

We measured the focal length of the microlens to be 175 ± 3 μm using setup shown in Fig. 2. SIL is used to image a line grating (10 μm linewidth) with an ordinary microscope as shown in (Fig. 7c). The magnification of SIL is calculated to be $M = 2.4 \pm 0.1$ which is to the expected value of $M = n_{SIL}^2 \simeq 2.3$.

3.2 Hybrid micro-optical elements

Many different methods are used to fabricate refractive and diffractive micro-optics,[36,37] yet there is still an outstanding issue to manufacture hybrid components in a single step procedure. The direct writing polymerization offers unmatched flexibility in production of bi-functional (and multi-functional) refractive-diffractive micro-optical devices, e.g., micro-lens with a phase grating on it can be manufactured directly (Fig. 8) as well as array of micro-lenses having differently oriented gratings (Fig. 9). Figure 10 shows examples of prisms (a) and an optical vortex generating grating (b), whose volume fraction of polymer is reduced by approximately 20% as compared with fully polymerized volume. A required 2π phase change over a single period of the grating can be achieved by a settle tuning of the volume fraction rather than the height change (or could both methods combined).

Light beam propagating through hybrid micro-optical element (Fig. 9) is focused by the spherical profile shape and diffracted due to the periodic lines on the surface. Zero to fourth order diffraction maxima were observed. In optical elements arrays diffraction gratings of neighboring lenses can be formed at a varying angle. This allows different light flow control variants to be achieved.

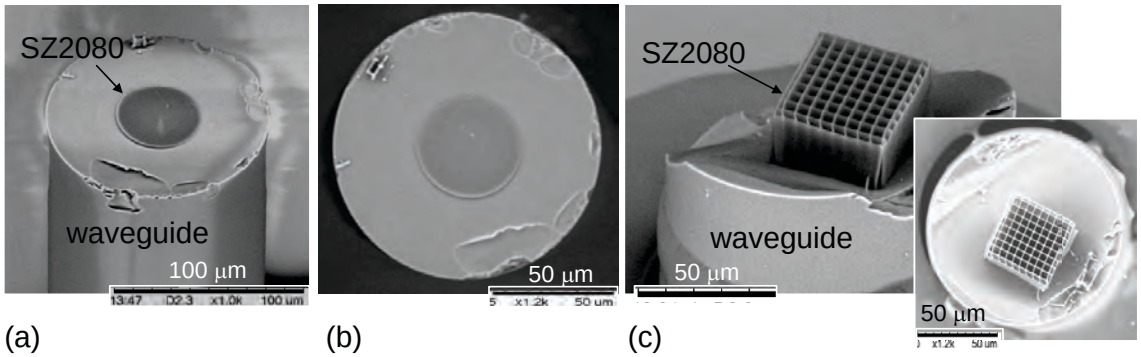

Figure 11. (a-b) SEM images of a micro-lens photo-polymerized on a tip of optical fiber. (c) A tilted micro-grating photo-polymerized directly on the tip of break-divided fiber. Inset shows top view of the structure.

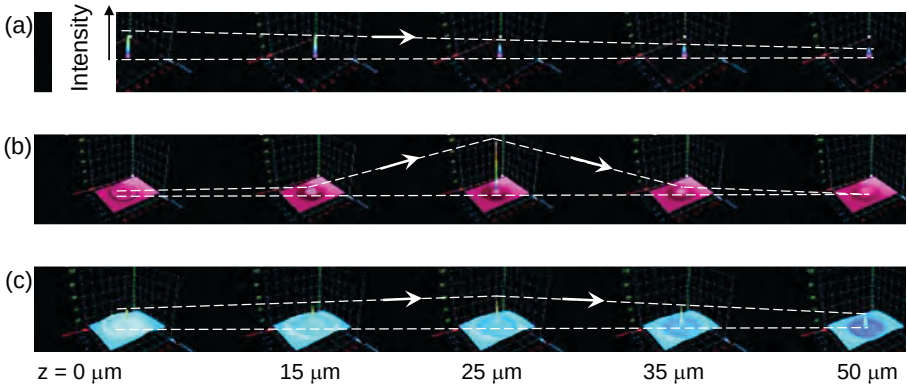

Figure 12. Measured 3D light intensity distributions (setup is shown in Fig. 2) along propagation from the tip of the fiber (a), along focusing path of a lens polymerized on the cover glass (b), and focusing of light by a polymerized lens on the tip of optical fiber (c). Position of $z = 0$ μm is the surface of fiber or cover glass. The dashed lines and arrows are eye guides for intensity flow along propagation.

3.3 Integrated micro-optical elements

There has been already shown that micro-optics on top of the fibers can increase their coupling or splicing efficiencies,[38] yet the task to manufacture desired micro-optical component on top of the fiber is not an easy one, starting from the precise positioning and centering the fiber.

Figure 11(a,b) shows a lens structure photo-polymerized on the tip of an optical fiber by direct laser write. The lens is functional as qualitatively illustrated in Fig. 12. By using setup shown in Fig. 1a, mounting and processing of fiber tip is a simple procedure. The tip of the fiber was dip coated by the resist before laser polymerization. Figure 11(c) illustrates a possibility to form a grating structure on a freshly broken and unpolished surface of the fiber tip.

3.4 Movable structures for micro-fluidics

Photonic crystal (PhC) templates can be polymerized by direct laser write in SZ2080 without attachment to the substrate as we reported earlier.[19,40*] Such structures can be pushed and pulled by laser tweezers inside the cage enclosure in which they were fabricated despite a large approximately 50 μm footprint of the PhC template. For manipulation by laser tweezers at 1064 nm wavelength, the polymerized structures were immersed in water between cover glasses as schematically shown in Fig. 13(a).

Figure 13(b,c) shows a peculiar imaging through a 3D photonic crystal structure. As the imaging plane moves from the entrance cover glass into the liquid one can recognize imaging of the front surface on the structure (as shown in (b)) and it is possible to make an image of the cage cap through the 3D structure (c) as focus is placed

*The photo-initiator was Irg. not Bis. as stated in ref.[19,40]

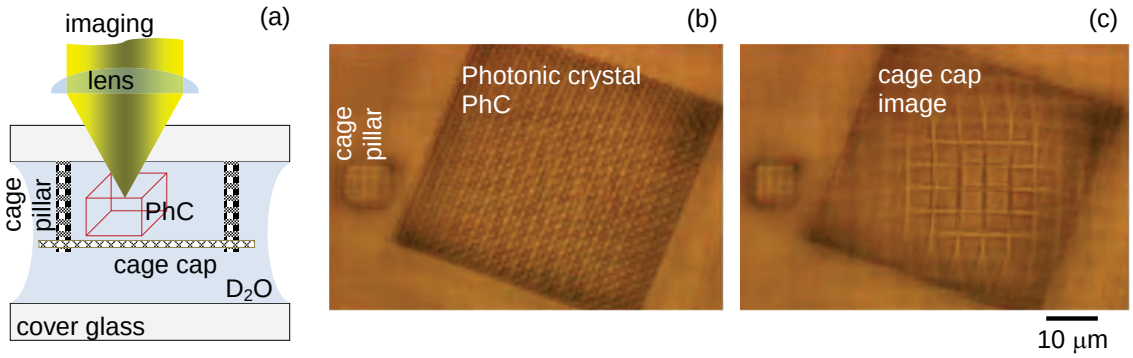

Figure 13. (a) Geometry of the sample: free spiral photonic crystal (PhC) structure fabricated inside a cage and immersed into heavy water for laser manipulation by laser tweezers. The cage cap is made by two-layer woodpile structure 22 μm above the substrate with pitch $d_{x,y} = 4$ μm; cage pillars are $4 \times 4 \times 25$ μm^3 $d_{x,y} = 1.2$ μm and $d_z = 0.7$ μm. The PhC is made of square spirals with periods $a = 1.0, d = 0.7, c = 1.4$ μm;[39] structure is made of 40 lateral and 8 axial periods.

further into the liquid. Note, the cage cap is out of image plane for the light which is not passing through the polymerized free-floating 3D structure. This is a direct evidence of the possibility to tailor dispersion via 3D structuring and control of volume fraction of the polymer. The 3D structure has slightly different refractive index causing dispersion of propagating light and, hence, a relay of the image plane. This can find applications in micro-fluidics and microscopy.

4. CONCLUSIONS

Formation of single and hybrid refractive-diffractive elements by fs-laser polymerization is demonstrated using a fast and practical combination of shell-formation and UV homogenization procedures. Such processing sequence speeds up the laser exposure by a factor $\sim 10^2$. The refractive index matching between cover glass and SZ2080 is used to form functional SIL lens by cap-polymerization. The imaging magnification increase by ~ 2.4 times, as expected for a fully formed SIL, is experimentally demonstrated. Arrays of such SIL lenses can be formed on cover glass or outside walls of micro-fluidic chambers and used for laser trapping.[41]

Integration of grating and lens on the tip of optical fiber is demonstrated. The presented examples of single micro-optical elements, possibility to make optical elements with combined functions and their integration into fiber optical elements adds new functionalities in the fields of opto-mechanics, opto-fluidics, and sensors.

By controlling volume fraction of the polymer, the effective refractive index of the polymerized structure can be tuned. Hence the same micro-optical elements would acquire different optical properties (refraction, focusing, and diffraction) in different fluids. In order to retrieve photo-polymerized structures with polymer fraction less than 0.5, as required for the photonic crystal templates, a critical point drying systems should be employed.

ACKNOWLEDGEMENTS

The research leading to these results has received funding from the Lithuanian State Science and Studies Foundation Grant B09/08 (Laser Micro-Processing with High Repetition Femtosecond Pulses) and EC's Seventh Framework Programme (LASERLAB-EUROPE, grant agreement No. 228334, OPTOBIO). H.G. is grateful for the Erasmus internship grant. Authors acknowledge Dr. M. Farsari for providing zirconium containing sol-gel hybrid photosensitive material SZ2080, Dr. A. Ovsianikov, A. Gaidukevičiūtė, and Prof. X. Gan for fruitful discussions; P. Gečys and A Maneikis for technical assistance.

REFERENCES

1. T. C. Chong, M. H. Hong, and L. P. Shi, "Laser precision engineering: from microfabrication to nanoprocessing," *Laser and Photon. Rev.* **4**(1), pp. 123–143, 2010.
2. K. Ikuta and K. Hirowatari, "Real three dimensional micro fabrication using stereo lithograpy and metal molding," in *Proc. IEEE MEM's-93*, pp. 42–47, 1993.

3. W. Denk, J. H. Strickler, and W. W. Webb, "Multi-photon laser scanning fluorescence microscopy," *Science* **248**, pp. 73–76, 1990.
4. S. Maruo, O. Nakamura, and S. Kawata, "Three-dimensional microfabrication with two-photon-absorbed photopolymerization," *Opt. Lett.* **2**(22), pp. 132 – 134, 1997.
5. V. Mizeikis, S. Juodkazis, A. Marcinkevicius, S. Matsuo, and H. Misawa, "Tailoring and characterization of photonic crystals," *J. Photochem. Photobiol. C* **2**(1), pp. 35–69, 2001.
6. S. Juodkazis, V. Mizeikis, and H. Misawa, "Three-dimensional microfabrication of materials by femtosecond lasers for photonics applications," *J. Appl. Phys.* **106**(5), p. 051101, 2009.
7. K. Kaneko, H.-B. S. X.-M. Duan, and S. Kawata, "Submicron diamond-lattice photonic crystals produced by multi-photon laser nanofabrication," *Appl. Phys. Lett.* **83**, pp. 2091–2093, 2003.
8. M. Straub and M. Gu, "Near-infrared photonic crystals with higher-order bandgaps generated by two-photon photopolymerization," *Opt. Lett.* **27**(20), pp. 1824–1826, 2002.
9. M. Deubel, G. V. Freymann, M. Wegener, S. Pereira, K. Busch, and C. M. Soukoulis, "Direct laser writing of three-dimensional photonic-crystal templates for telecommunications," *Nature Mater.* **3**, pp. 444–447, July 2004.
10. J. Serbin, A. Ovsianikov, and B. Chichkov, "Fabrication of woodpile structures by multi-photon polymerization and investigation of their optical properties," *Opt. Express* **12**, pp. 5221–5228, 2004.
11. V. Mizeikis, K. K. Seet, S. Juodkazis, and H. Misawa, "Three-dimensional woodpile photonic crystal templates for infrared spectral range," *Opt. Lett.* **29**(17), pp. 2061 – 2063, 2004.
12. R. Guo, S. Xiao, X. Zhai, J. Li, A. Xia, and W. Huang, "Micro lens fabrication by means of femtosecond two photon photopolymerization," *Opt. Express* **14**, pp. 810–816, 2006.
13. Q.-D. Chen, D. Wu, L.-G. Niu, J. Wang, X.-F. Lin, H. Xia, and H.-B. Sun, "Phase lenses and mirrors created by laser micronanofabrication viamulti-photon photopolymerization," *Appl. Phys. Lett.* **91**(17), p. 171105, 2007.
14. Y. Li, Y. Yu, L. Guo, S. Wu, C. Chen, L. Niu, A. Li, and H. Yang, "High efficiency multilevel phase-type fresnel zone plates produced by multi-photon polymerization of SU-8," *J. Opt.* **12**(3), p. 035203, 2010.
15. M. Malinauskas, H. Gilbergs, A. Žukauskas, V. Purlys, D. Paipulas, and R. Gadonas, "A femtosecond laser-induced multi-photon photopolymerization technique for structuring microlenses," *J. Opt.* **12**(39), p. 035204, 2010.
16. J. Serbin, A. Egbert, A. Ostendorf, B. N. Chichkov, R. Houbertz, G. Domann, J. Schulz, C. Cronauer, L. Frohlich, and M. Popall, "Femtosecond laser-induced two-photon polymerization of inorganic-organic hybrid materials for applications in photonics," *Opt. Lett.* **28**(5), pp. 301–303, 2003.
17. H. Nishiyama, J. Nishii, M. Mizoshiri, and Y. Hirata, "Microlens arrays of high-refractive-index glass fabricated by femtosecond laser lithography," *Appl. Surf. Sci.* **255**(24), pp. 9750–9753, 2009.
18. K. Yamasaki, S. Juodkazis, S. Matsuo, and H. Misawa, "Three-dimensional microchannels in polymers: one step fabrication," *Appl. Phys. A* **77**, pp. 371–373, 2003.
19. Q. Sun, S. Juodkazis, N. Murazawa, V. Mizeikis, and H. Misawa, "Freestanding and movable photonic microstructures fabricated by photopolymerization with femtosecond laser pulses," *J. Micromech. Microeng.* **20**, pp. 035004/1–5, 2010.
20. R. Houbertz, L.Fröhlich, M. Popall, U. Streppel, P. Dannberg, A. Bräuer, J. Serbin, and B. N. Chichkov, "Inorganic-organic hybrid polymers for information technology: from planar technology to 3D nanostructures," *Adv. Eng. Mater* **5**(8), pp. 551–555, 2003.
21. A. Ovsianikov, J. Viertl, B. Chichkov, M. Oubaha, B. MacCraith, I. Sakellari, A. Giakoumaki, D. Gray, M. Vamvakaki, M. Farsari, and C. Fotakis, "Ultra-low shrinkage hybrid photosensitive material for two-photon polymerization microfabrication," *ACS Nano* **2**(11), pp. 2257–2262, 2008.
22. J. L. Li, B. Jia, G. Zhou, and M. Gu, "Fabrication of three-dimensional woodpile photonic crystals in a PbSe quantum dot composite material," *Opt. Express* **14**(22), pp. 10740–10745, 2006.
23. M. Farsari, A. Ovsianikov, M. Vamvakaki, I. Sakellari, D. Gray, B. N. Chichkov, and C. Fotakis, "Fabrication of three-dimensional photonic crystal structures containing an active nonlinear optical chromophore," *Appl. Phys. A* **93**, pp. 11–15, 2008.

24. T. Woggon, T. Kleiner, M. Punke, and U. Lemmer, "Nanostructuring of organic-inorganic hybrid materials for distributed feedback laser resonators by multi-photon polymerization," *Opt. Express* **17**(4), pp. 2500–2507, 2009.
25. C. R. Mendonca, D. S. Correa, F. Marlow, T. Voss, P. Tayalia, and E. Mazur, "Three-dimensional fabrication of optically active microstructurescontaining an electroluminescent polymer," *Appl. Phys. Lett.* **95**(11), p. 113309, 2009.
26. A. Žukauskas, M. Malinauskas, L. Kontenis, V. Purlys, D. Paipulas, M. Vengris, and R. Gadonas, "Organic dye doped microstructures for optically active functional devices fabricated via two-photon polymerization technique," *Lithuanian J. Phys.* **50**(11), pp. 55–61, 2010.
27. A. Ovsianikov, A. Gaidukeviciute, B. Chichkov, M. Oubaha, B. MacCraith, I. Sakellari, A. Giakoumaki, D. Gray, M. Vamvakaki, M. Farsari, and C. Fotakis, "Multi-photon polymerization of hybrid sol-gel materials for photonics applications," *Laser Chem.* **2008**, pp. 1–7, 2008.
28. A. Ovsianikov, A. Gaidukeviciute, B. N. Chichkov, M. Oubaha, B. D. MacCraith, I. Sakellari, A. Giakoumaki, D. Gray, M. Vamvakaki, M. Farsari, and C. Fotakis, "Two-photon polymerization of hybrid sol-gel materials for photonics applications," *Laser Chem.* **2008**, p. ID 493059, 2008.
29. M. Malinauskas, A. Žukauskas, G. Bičkauskaitė, R. Gadonas, and S. Juodkazis, "Mechanisms of three-dimensional structuring of photo-polymers by tightly focussed femtosecond laser pulses," *Opt. Express* **18**(10), pp. 10209–10221, 2010.
30. T. Kondo, S. Juodkazis, and H. Misawa, "Reduction of capillary force for high-aspect ratio nanofabrication," *Appl. Phys. A* **81**(8), pp. 1583 – 1586, 2005.
31. H. Sun and S. Kawata, "Multi-photon photopolymerization and 3D lithographic microfabrication," *Adv. Polym. Sci.* **170**, pp. 169–273, 2004.
32. M. Malinauskas, V. Purlys, M. Rutkauskas, A. Gaidukeviciute, and R. Gadonas, "Femtosecond visible light induced two-photon photopolymerization for 3D micro/nanostructuring in photoresists and photopolymers," *Lithuanian J. Phys.* **50**(2), 2010 (in press).
33. A. Marcinkevicius, V. Mizeikis, S. Juodkazis, S. Matsuo, and H. Misawa, "Effect of refractive index-mismatch on laser microfabrication in silica glass," *Appl. Phys. A.* **76**, pp. 257–260, 2003.
34. S. M. Mansfield and G. S. Kino, "Solid immersion microscope," *Appl. Phys.Lett.* **57**(24), pp. 2615–2617, 1990.
35. M. Yoshita, M. Baba, and H. Akiyama, "Improved high collection efficiency in fluorescence microscopy with a weierstrass-sphere solid immersion lens," *Jpn. J. Appl. Phys.* **41**, pp. 858–860, 2002.
36. A. Cannistra and T. Suleski, "Characterization of hybrid molding and lithography for su-8 micro-optical components," *J. Micro/Nanolith. MEMS MOEMS* **9**(1), p. 013025, 2010.
37. S. Sinzinger and M. Testorf, "Transition between diffractive and refractive micro-optical components," *Appl. Opt.* **34**(26), pp. 5970–5976, 1995.
38. F. Schiappelli, R. Kumar, M. Prasciolu, D. Cojoc, S. Cabrini, M. D. Vittorio, G. Visimberga, A. Gerardino, C. Degiorgio, and E. D. Fabrizio, "Efficient fiber-to-waveguide coupling by a lens on the end of the optical fiber fabricated by focused ion beam milling," *Microelectron. Eng.* **73-74**, pp. 397–404, 2004.
39. K. K. Seet, V. Mizeikis, S. Matsuo, S. Juodkazis, and H. Misawa, "Three-dimensional spiral - architecture photonic crystals obtained by direct laser writing," *Adv. Mat.* **17**(5), pp. 541 – 545, 2005.
40. Q. Sun, S. Juodkazis, N. Murazawa, V. Mizeikis, and H. Misawa, "Femtosecond laser photopolymerization of photonic and free-movable microstructures in sol-gel hybrid resist," p. 75910K, Proc. SPIE vol. 7591, 2010.
41. H. Misawa and S. Juodkazis, "Photophysics and photochemistry of a laser manipulated microparticle," *Prog. Polym. Sci.* **24**, pp. 665–697, 1999.